

Figure 1: Schematic diagram of an electron bombardment ion source. From reference [2]

1 Mass Spectroscopy

Mass spectrometers that work in vacuum consist of three parts: (1) an ionizer, (2) a mass selector, and (3) a detector. These will be considered separately and then followed with a series of example applications.

1.1 Ionization

The most common way to ionize a gas phase atom or molecule is by electron impact. This is the same approach employed in the Bayard-Alpert ionization gauge discussed in the section on pressure measurement. In the ionizer of a mass spectrometer, charged particle optics are constructed to produce both an electron beam and to extract the resulting ions and deliver them to the mass selector. A schematic diagram of an electron bombardment ion source is shown in figure 1; the size is about 1 inch. Electrons are boiled off a heated filament and accelerated across a gap. The same sort of electron kinetic energies used in the ion gauge are employed, typically around 70 eV. A table of electron impact ionization cross sections for selected species was given in section 1 and is reproduced here in Table 1. Ions formed are extracted perpendicular to the electron beam and accelerated to form a beam with a well defined kinetic energy.

The electron impact ionization process can be rather destructive, particularly for larger molecules such as might be of interest in biochemistry or biology. Getting these heavier species into the gas intact can also be problematic. A popular alternative is illustrated in figure 2 and is called electrospray ionization. It has the advantage of a relatively benign vaporization step and very gentle ionization. Droplets of solvent containing the species of interest are injected into a vacuum chamber through a capillary needle. The needle is held at a high voltage with respect to ground so the drops have a net charge on them. As the drops travel through the chamber, the solvent evaporates concentrating the charge on the drop. As the charge increases the surface tension can no longer hold the drop together against the Coulomb repulsion and the drops explode into smaller drops. This process repeats and some of the molecule of interest end up as bare ions.

Table 1: Experimental Total Ionization Cross Sections at 70 eV Electron Energy (Normalized to Nitrogen)

Gas	Relative Cross Section
H ₂	0.42
He	0.14
CH ₄	1.57
Ne	0.22
N ₂	1.00
CO	1.07
C ₂ H ₄	2.44
NO	1.25
O ₂	1.02
Ar	1.19
CO ₂	1.36
N ₂ O	1.48
Kr	1.81
Xe	2.20
SF ₆	2.42

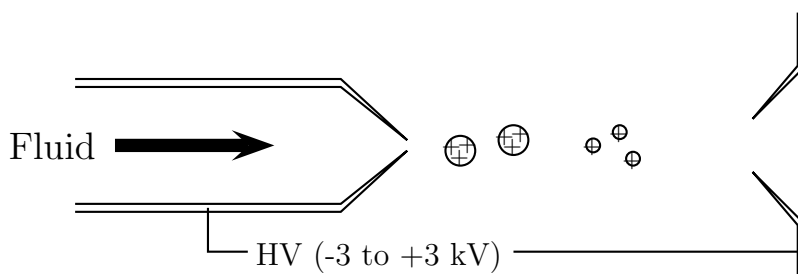


Figure 2: Schematic of an electrospray ion source.

Problem: A drop of water has a net charge of $-q$ on it. Assume the charge is distributed uniformly on the surface of the drop and the interior of the drop is charge neutral. The drop is held together by surface tension; the surface tension of water is 72 dynes/cm. The surface tension times the surface area is an energy. As the drop evaporates, this energy drops. Estimate the size at which the drop becomes unstable by equating the electrostatic potential energy to the energy holding the drop together.

A related technique is called matrix assisted laser desorption and ionization (MALDI) has also been developed. Here the molecule is frozen in a rare gas solid which is then rapidly vaporized using a pulsed laser. In effect, the rapid vaporization step leaves little time for decomposition to take place. Some fraction of the species is also ionized.

1.2 Mass Selection

Once a beam of charged particles are produced in the gas phase, magnetic and/or electric fields can be used to manipulate their trajectories. Since the interactions with these fields typically depends of the ratio of the ions charge to mass (q/m) a mass selection can be realized.

The conceptually simplest of these has the ion beam with a well defined

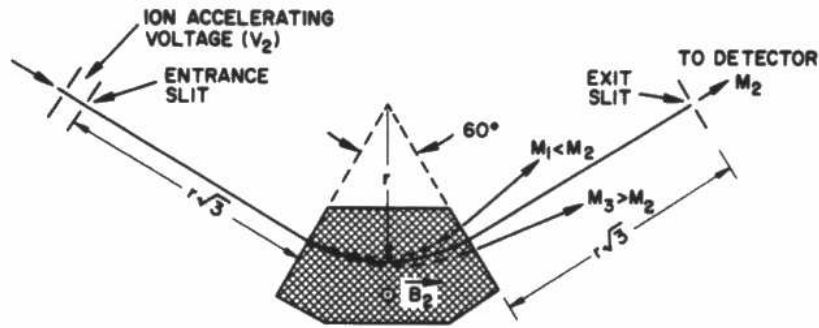


Figure 3: A 60 magnetic sector mass spectrometer with symmetric entrance and exit slits. From reference [1].

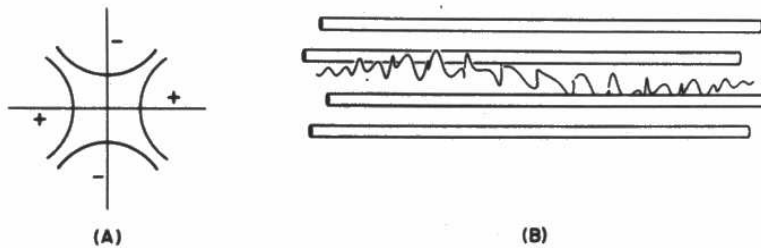


Figure 4: Quadrupole mass filter: (a) Idealized hyperbolic cross section of the electrodes. (b) Three dimensional representation of a stable ion path. From reference [1].

kinetic energy Lorenz force deflects the ion beam. This is illustrated in figure 3 for the most common implementation in which the ion of interest is deflected by 60° . The distribution in final angle then maps to a spectrum of q/m , and is defined by suitably placed entrance and exit slits. This mass selection is typically used in a device dedicated to detection of a single ion, such as in a Helium leak detector.

By far the most common mass selector in laboratory applications is the quadrupole mass filter. This is a compact and reliable device routinely used to many applications such as residual gas analysis and composition analysis. The layout of the four rods is shown in figure 4 and the electric fields are shown in figure 5. The mass range and mass resolution of a quadrupole is determined by the diameter and length of the rods: typically, for unit mass resolution from 1-200 amu, the rods are about 1 cm in diameter and 15 cm long.

The combination of a DC voltage (U) and an AC voltage in the RF range ($V \cos \omega t$) results in a band pass filter based on q/m . The amplitudes U and V are varied together to tune the q/m that is passed through. Ions inside the rods have both a long wavelength and short wavelength component to their motion. Only one particular q/m ratio will arrive at the other end of the quadrupole rods on the axis. An aperture then admits those ions to a detector.

The equations of motion are [2]

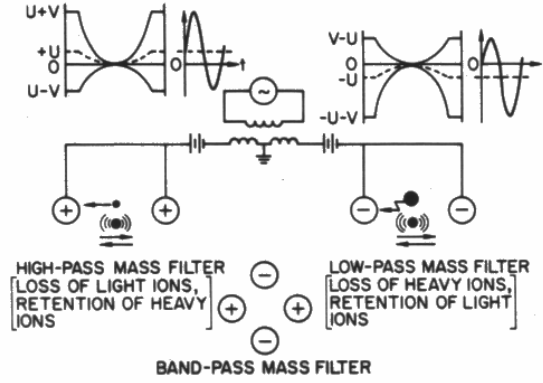


Figure 5: Electric fields in a quadrupole mass filter. From reference [1].

$$\ddot{x} + \frac{2ne}{mr_0^2}(U + V \cos \omega t)x = 0 \quad (1)$$

$$\ddot{y} - \frac{2ne}{mr_0^2}(U + V \cos \omega t)y = 0 \quad (2)$$

$$\ddot{z} = 0 \quad (3)$$

These are the so-called Mathieu membrane equations and are discussed in terms of regions of stability where the ion motion does not diverge from the central axis.

If one of the rods is bent into a ring and the other turned into top and bottom electrodes the configuration is termed a quadrupole ion trap and is used to hold ions for long time spectroscopic observation.

An alternative method to separate species by charge to mass ratio involves using a pulsed source of ions. The ions are accelerated through a given potential difference. This produces a batch of ions all having the same kinetic energy. These ions are allowed to fly freely for some distance and are then separated in time with the heavier ions arriving at a detector later than the light ones. The flight time is proportional to the square root of the mass. The detector signal has to be recorded as a function of time. This is called a time-of-flight (TOF) mass spectrometer. An example of this type of analyzer is shown in section 1.4.2.

1.3 Detection

The simplest way to detect an ion is to let it neutralize at a metal surface and measure the current required. This is shown in figure 6 and is called a Faraday cup since sometimes it is shaped like a cup to minimize back scatter of secondary electrons. In the case of a Faraday cup all amplification has to be done in external electronics, so it is used when the ion current is relatively large. For lower ion flux, amplification is built in to the detector. A positive voltage is applied to the Faraday cup to deflect the ions into the first element of a dynode chain. A negative high voltage (usually in the range of 1-3 kV) on this element accelerates the ion into the surface and secondary electrons are emitted. A series of dynodes, each biased more positive than the previous, is arranged so that the secondary electrons from the previous element will be accelerated into it and produce even more secondaries. The final electrode collects the electron bunch

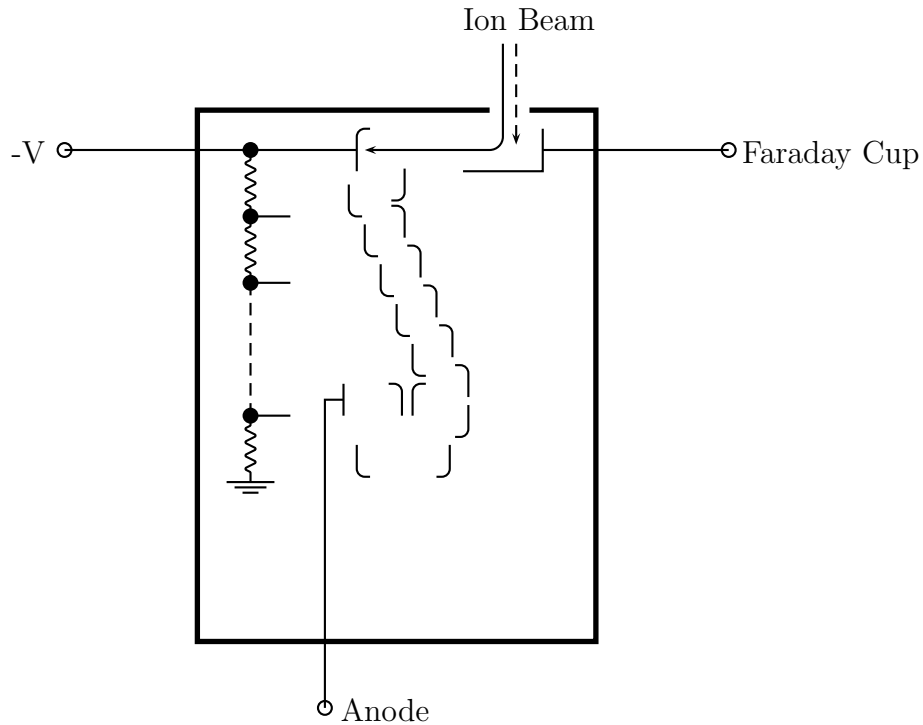


Figure 6: Combination Faraday cup-electron multiplier detector.

where it is observed as a pulse. The pulse corresponding to the arrival of one ion is typically only a few ns in duration with on the order of 10^5 electrons in it and can be readily measured, so this detector is often used in a pulse counting mode instead of a continuous current mode. A drawback of this kind of electron multiplier is that the bias voltages for each element have to be generated in a chain of resistors, and this chain draws a fair amount of current from the negative supply.

A more modern implementation of the electron multiplier is shown in figure 7. Here the discrete chain of dynodes is replaced by a continuous tube (often in the form of a spiral, like a pig's tail). The tube is made of glass impregnated with lead to produce a desired resistance between the cathode and anode. Thus there is a continuous voltage drop along the tube to accelerate the electrons; the curvature ensures that the accelerated electrons will undergo multiple, secondary producing, collisions during transit. These multipliers cost a few hundred dollars, are a few cm in size and are common in all charged particle detectors. The resistance of the semiconducting tube is often quite high, so the device consumes less power than the discrete version in figure 6. This makes them the detector of choice, for example, on spacecraft.

An further development of the electron multiplier uses an array of microscopic channels called a CEMA for channel electron multiplier array, that can form an image of a source of charged particles. This is illustrated in figure 8. Each channel is made from semiconducting lead glass with a high voltage applied between the ends like before. A large number of glass optical fibers are bundled together, drawn out to decrease their cross section; then the core of the fiber is dissolved away leaving hollow tubes, and the cut into slices. The faces

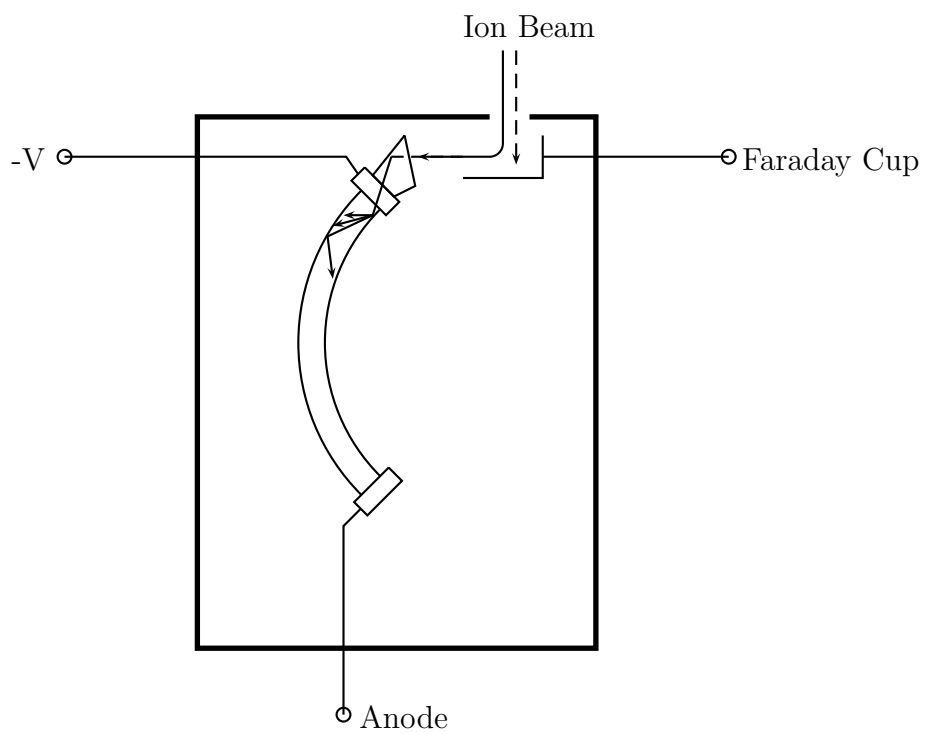


Figure 7: Channeltron (Galileo Electro-Optics) electron multiplier incorporated into a mass analyzer.

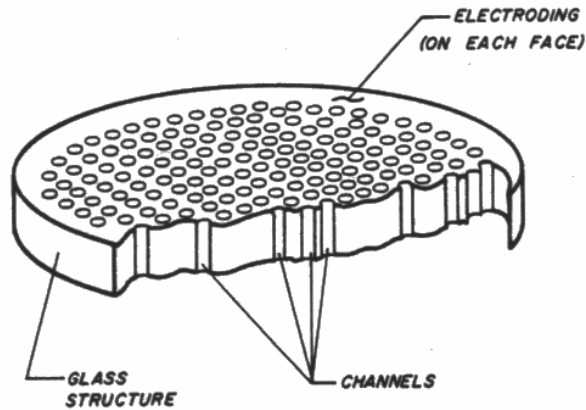


Figure 8: Cutaway view of a microchannel plate (Galileo Electro-Optics).

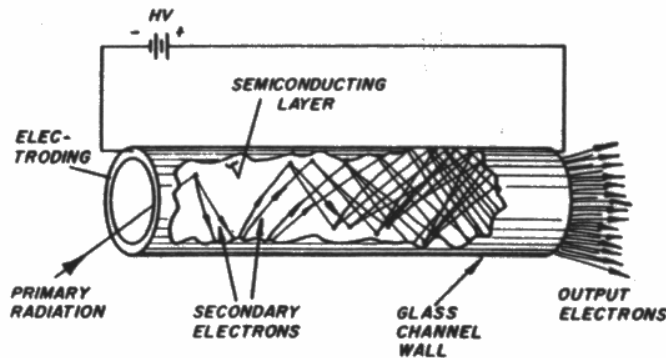


Figure 9: Schematic view of a single channel of a microchannel plate.

of the plate are coated with metal to provide a conducting path for the bias. Each slice is about 2 mm thick and usually 25 or 50 mm in diameter. Each fiber ends up about $12\ \mu\text{m}$ in diameter with a channel about $10\ \mu\text{m}$ across. The channels are tilted with respect to the plate normal so that incident charged particles do not pass straight through. The plate has a gain on the order of 10^3 to 10^4 and often two of them are stacked together. They can be used in image intensifiers (for example night vision goggles), of in situations where large dynamic range in ion flux is needed. Since each channel operates as a separate multiplier, and there are a large number of channels, the device is linear up to fairly large incident flux.

1.4 Examples and Applications

1.4.1 Laboratory Applications

A simple example of a mass spectrometer application in a physics laboratory is shown in figure 10. This is what mine might see in a “high vacuum” apparatus after pump down without any particular handling with regards cleanliness, and without any bake out. This spectrum is typical of what might be recorded with a commercial, electron impact, quadrupole mass spectrometer with a Faraday cup or electron multiplier detector. The mass to charge ratio goes up to about

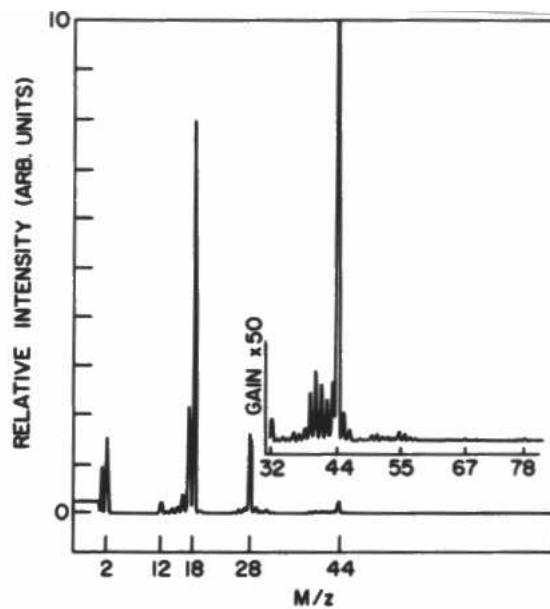


Figure 10: Mass scan taken on a small oil diffusion pumped chamber with an RF quadrupole instrument. From reference [1].

100.

Prominent peaks in the spectrum appear at masses 2, 18, 28 and 44. Mass 2 is H_2^+ , 18 is H_2O^+ and 44 is CO_2^+ . Several additional features are worth commenting on: there is a peak at mass 1 corresponding to H^+ which results from the dissociation of H_2 . Since the energy of the electrons in the ionizer is about 70 eV, and the bond strength of H_2 is only 4.5 eV this peak should not be surprising. This concept also explains the peaks below mass 18: mass 17 is OH^+ and 16 is O^+ . Now we come to the peak at 28. This could be (amongst other things) N_2 or CO . The key to differentiating between these two is to look for the fragments. There is a peak at mass 12 which is C^+ but not one for mass 14 which would be N^+ , so the mass 28 peak can be assigned to CO . This process illustrates the steps one goes through to interpret a spectrum like that shown. However, if this represents the residual gas in a vacuum chamber after pumping down from atmospheric pressure, why is the composition so different from air (roughly 78% N_2 , 21% O_2 , 0.4% Ar and traces of other gases)? This point will be addressed in section 3 on surface science.

A second example of a mass spectrum is shown in figure 11 for carbon monoxide. Such a plot is called a *cracking pattern*. This spectrum is plotted on a log scale to illustrate the sensitivity and dynamic range of a spectrometer with an electron multiplier as detector. The peak amplitude is normalized to 100 for the strongest feature, in this case the *parent* mass, CO^+ at 28. Visible are the naturally occurring isotopes $^{13}\text{C}^{16}\text{O}^+$ at 29 and $^{12}\text{C}^{18}\text{O}^+$ at 30 as well as the fragments $^{12}\text{C}^+$ at 12 and $^{16}\text{O}^+$ at 16. A new feature not readily apparent in figure 10 but made visible on the log plot, is the appearance of multiply charged ions at one-half values of m/q : $^{12}\text{C}^{++}$ at $m/q = 6$ and $^{16}\text{O}^{++}$ at 8. Also seen is the doubly charged molecular ion $^{12}\text{C}^{16}\text{O}^{++}$ at m/q of 14. Relatively few molecules can loss two electrons and not fragment, CO is one of these. On a side note, it is ^{14}C that is used in carbon dating, so one wonders why it does not appear in this spectrum. The answer is that the steady state abundance of ^{14}C in the earth's atmosphere is only 1.3×10^{-12} that of ^{12}C , so the measley 6

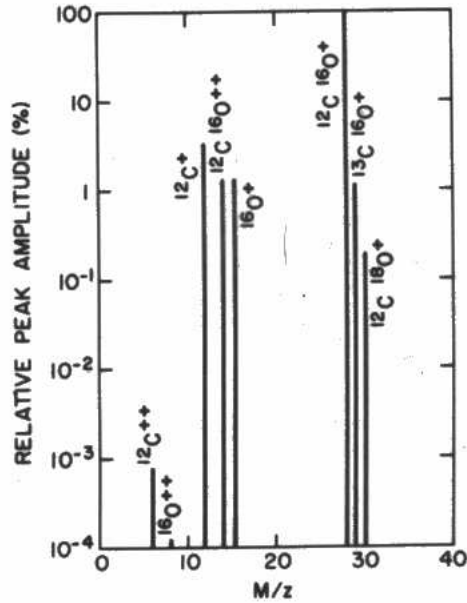


Figure 11: Cracking pattern of CO illustrates dissociative ionization, isotopic and doubly ionized peaks. From reference [1].

orders of magnitude represented in figure 11 is not going to cut it.

A third sample mass spectrum showing another example of isotopes is shown for argon in figure 12. This spectrum is again plotted on a log scale and shows a triplet of doubly charge ions matching the relative intensity pattern of the singly charged ions. What is the origin of the isotopes in a spectrum like this? The isotopes are often made by cosmic ray processes in the atmosphere. In some cases for long lived isotopes, the pattern reflects the cumulative, long term kinetics of production and decay as the cosmic ray and earth's natural radioactivity have evolved on geological time scales. For example, much of what is known about the past composition of the earth's atmosphere is based on isotopic analysis of gasses trapped in ice cores in Greenland and Antarctica. The acquisition and analysis of such ice cores and other relics of earlier times as well as more recent samples is the basis of much of the field of geochemistry.

1.4.2 Space Applications

An increasing amount of information is being gathered on parts of our solar system other than the earth. In particular data has been acquired for Mars and in experiments underway at the present time, for Saturn's moon Titan. The composition of the lower Martian atmosphere is given in table 1.4.1. This data is from the Viking landers in the 1970's. Again, the dynamic range is impressive.

Also measured by the mass spectrometer aboard the Viking landers was the isotope distribution of the Martian atmosphere. This is shown in table 1.4.2 in comparison with the same species on earth. The differences are apparent and the large (factor of 10) ratio for Argon remains to be explained. The accurate measurement of the isotope ratios on Mars and the appearance of several marked differences with earth has allowed for definitive identification of a number of meteorites found in Antarctica as being of Martian origin. The analysis of these meteorites generated some controversy when it was claimed that they contained evidence of life [3]. Prevailing opinion is now that that conclusion was wrong,

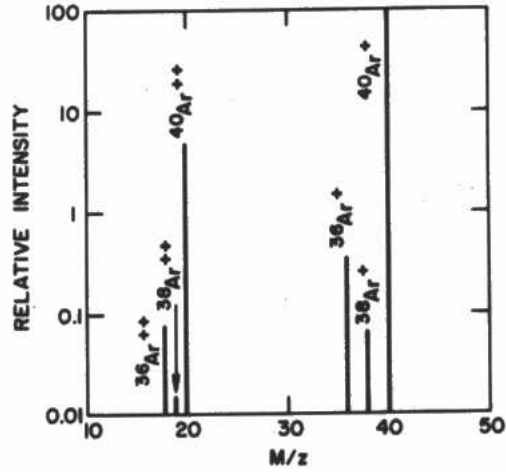


Figure 12: The argon cracking pattern illustrates isotopic mass differences (three isotopes) and two degrees of ionization (single and double). From reference [1].

Table 2: Chemical composition of the lower Martian atmosphere. From Owen et al., JGR **82** 4635 (1977).

Gas	Proportion
Carbon Dioxide	95.32%
Nitrogen	2.7%
Argon	1.6%
Oxygen	0.13%
Carbon Monoxide	0.07%
Water Vapor	0.03%
Neon	2.5 ppm
Krypton	0.3 ppm
Xenon	0.08 ppm
Ozone	0.03 ppm

Table 3: A comparison of isotope ratios in atmospheric gases between the Martian and Earth atmospheres. From Becker and Pepin, Earth and Planetary Science Letters **69** 225 (1984).

Ratio	Earth	Mars
$^{12}\text{C}/^{13}\text{C}$	89	90
$^{14}\text{N}/^{15}\text{N}$	277	165
$^{16}\text{O}/^{18}\text{O}$	499	500
$^{40}\text{Ar}/^{36}\text{Ar}$	292	3000
$^{129}\text{Xe}/^{132}\text{Xe}$	0.97	2.5

Table 4: Comparison of isotope ratios for gases from earth, Mars and several meteorites found in Antarctica. From Owen et al., JGR **82** 4635 (1977).

	$^{40}\text{Ar}/^{36}\text{Ar}$	$^{129}\text{Xe}/^{132}\text{Xe}$
EETA 79001 samples		
C1	2300 ± 190	-
C2	2440 ± 170	2.231 ± 0.0037
Mars	3050 ± 1000	2.5 (1.5-4.5)
Earth	296	0.983

but the Martian origin of the meteorites was not in question: the isotope ratios nailed that down. The isotope data is compared in Table 1.4.2 and in Figure 13.

One of the primary instrument packages on the Cassini mission to Saturn is shown in figure 14. The three separate units comprising the CAPS unit are designed to measure different components of Saturn's magnetosphere: electrons, ions independent of chemical identity, and ions with chemical identification. The latter detector is the IMS for ion mass spectrometer. Ions entering within a specified angular range are filtered in an electrostatic analyzer (ESA) consisting of two hemispheres with a potential bias established between them. Ions with the right charge to mass ratio and within a certain energy range will pass between the hemispheres and then be accelerated into thin carbon foils. On passage through the foils, a fraction of the molecular ions will be fragmented into atomic ions. This ions run up a hill consisting of a electric field gradient, turn around and hit a MCP detector. Electrons generated in the foil are accelerated by this electric field and hit an MCP detector at the bottom and generate a trigger signal. The ion arrival at the upper MCP is later, and the time of arrival translates to the mass of the ion. One advantage of this type of mass spectrometer is that it can distinguish between CO and N₂. This is shown in the sample spectrum in figure 15. The MCP for detecting the ions is segmented like a pie so that some information is gathered concerning the azimuthal angle of incidence (with respect to the plane of figure 14) of the original ion that entered the instrument.

The electric field as a function of radial position r between the two hemispheres in an electrostatic analyzer is given by

$$E = \frac{\Delta U}{r^2} \left(\frac{R_1 R_2}{R_2 - R_1} \right) \quad (4)$$

where the hemispheres have radii R_1 and R_2 and ΔU is the potential difference between them. The equations of motion for a charged particle are

$$m\ddot{r} - mr\dot{\theta}^2 + \frac{k}{r^2} = 0 \quad (5)$$

$$2mrr\dot{\theta} + mr^2\ddot{\theta} = \frac{d}{dt} (mr^2\dot{\theta}) = 0. \quad (6)$$

where

$$k = Q\Delta U \left(\frac{R_1 R_2}{R_2 - R_1} \right). \quad (7)$$

The solutions to these equations are Keplerian elliptical orbits.

Problem: The radii for the IMS on the Cassini CAPS are 98.75 mm and 101.25 mm. If a CO⁺ ion enters the spectrometer with a kinetic energy of 20 eV, what

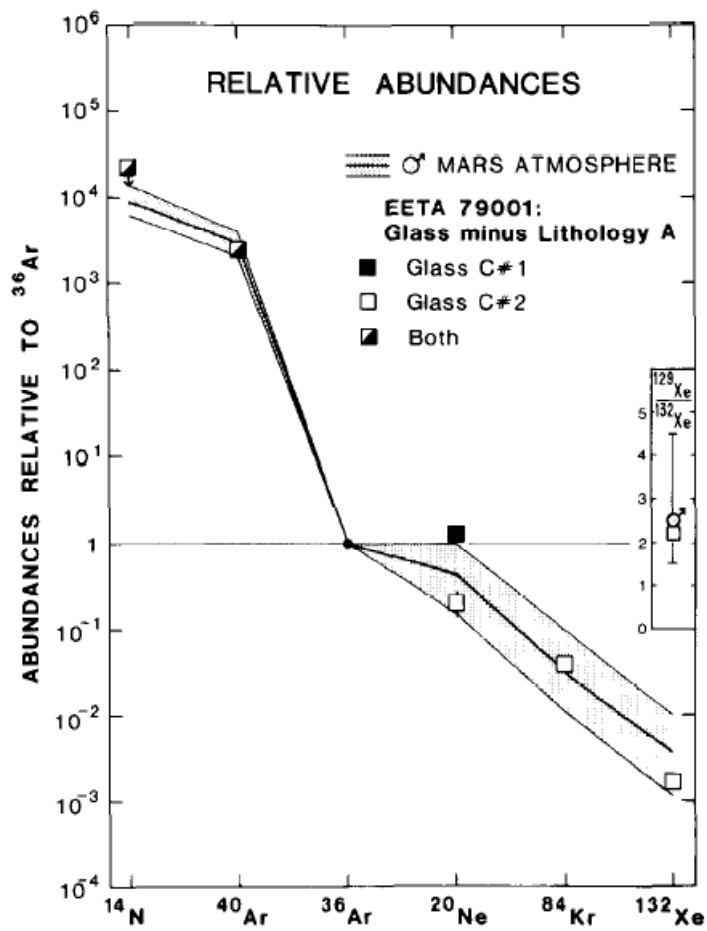


Fig. 3. Relative abundances of trapped noble gas and nitrogen isotopes in EETA 79001, compared with data on the martian atmospheric composition (Table 5).

Figure 13:

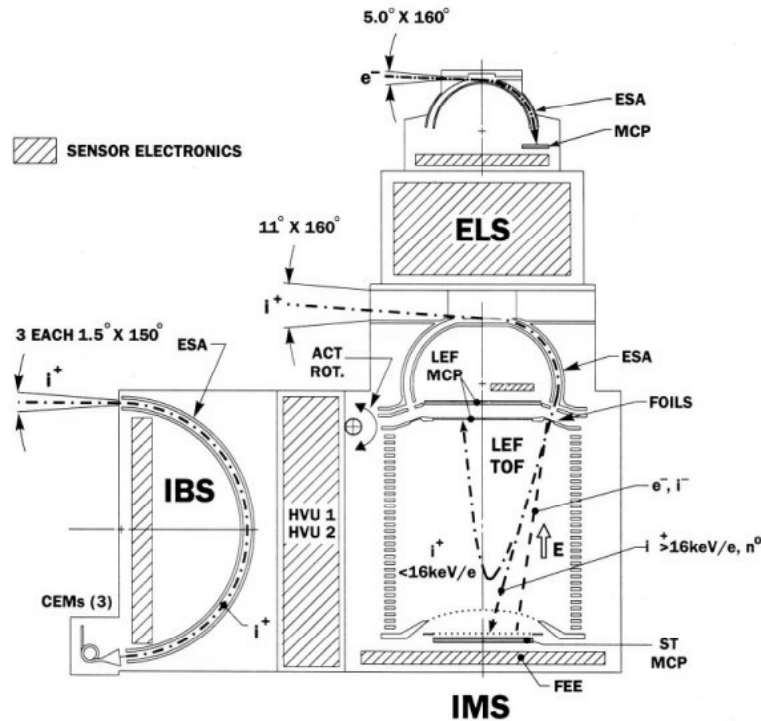


Figure 1. Schematic diagram of CAPS sensor optics. All 3 sensor fields-of-view (FOV) are fan-shaped with the long (polar angle) axis of the IMS, ELS and one IBS fan perpendicular to the plane of the page. The center of rotation of the FOVs is indicated by the ACT ROT label at the center of the figure. Rotation is defined to be in the azimuthal plane of CAPS optics. Heavy dot-dash lines indicate central particle rays in the three optical systems.

Figure 14: CAPS sensors, from Young et al., Geophys. Monograph 102, 237 (1998).

voltages on the spheres will transmit this ion? Assume that the initial velocity of the ion is tangential to the hemispheres radii; then the problem is easy. Just balance the Coulomb and 'centrifugal' force terms in equation 5, then \ddot{r} will be zero and since initially \dot{r} is zero, $\dot{\theta}$ will be zero and the ion will just follow a circular orbit. What range of kinetic energies will be transmitted? This is harder and requires you to integrate the equations of motion and see what the final r (when $\theta = \pi$) will be for different energies.

A different type of mass analyzer with much higher resolution is shown in figure 16 and is based on the charge-to-mass dependence of the cyclotron frequency of an ion in a magnetic field. Ions are formed by any of the usual techniques, for example electron impact, and extracted into a region of uniform magnetic field where they undergo uniform circular motion with a frequency of $\omega_c = qB/m$, typically in the Mhz range. Radio frequency pulses at this frequency are used to increase the radius of the motion to just under the size of the apparatus. This process also causes the ions to bunch up into a pulse. As the bunch circulates, image currents are detected in the receiver plates (see the figure) and the image currents are measured as a function of time. The Fourier transform of the signal is then calculated. Ions can be held in such a system for 10^7 - 10^8 cycles meaning that ω_c can be determined very accurately. The observation time is usually limited by vacuum, that is by collisions with

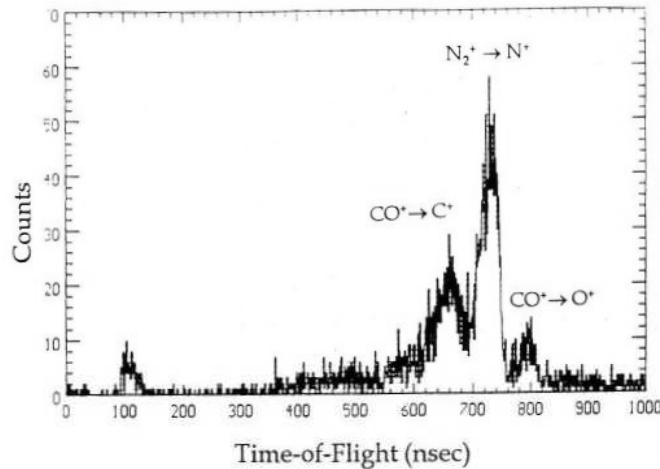


Figure 6. Timing spectra for a 10keV ion beam of mass 28amu obtained using laboratory electronics.

Figure 15: Sample CAPS mass spectrum, from Nordholt et al., Geophys. Monograph 102, 209 (1998).

FOURIER TRANSFORM ION CYCLOTRON RESONANCE

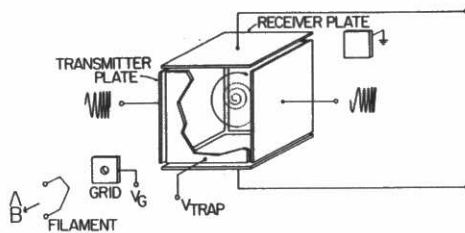


Figure 16: Schematic of the cubic ion cyclotron resonance cell. Ions are formed by an electron beam pulse, and the coherent motion of ions undergoing resonance is detected by image currents induced in the receiver plates. From reference [2].

background gas.

An example of a so-called Fourier transform mass spec (FTMS) is shown in figure 17 in the region of mass-to-charge ratio 28. Three ions with nominally equal masses (N_2^+ , CO^+ and C_2H_4) are resolved. The difference in mass between N_2^+ and CO^+ is essentially a measure of the binding energy in the nuclei since both have the same number of both protons and neutrons. The best FTMS instruments constructed have resolutions approaching 10^9 , meaning that they are close to resolving the energy of *chemical* bonds.

A more complicated application of mass spectroscopy is shown in figure 18. The compound shown is a steroid and the 4 ring structure is characteristic of this class of comunds. Such spectra might be recorded, for example, in the course of drug tests for athletes where high confidence in the identification of a substance is obviously critical. Several points are worth noting. First, the parent mass peak is very small or nonexistent in the deuterated case, so the fragment distribution is key. Second, there are prominent peaks associated with the loss of specific groups, called ligands. Thus there is a peak at m-29, where

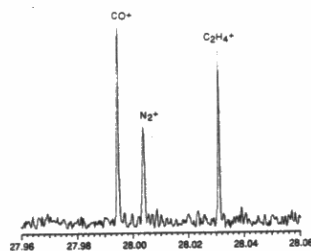


Figure 17: High resolution FT mass spectrum obtained at 0.6 T. The three peaks correspond to CO⁺ (m/q 27.9944), N₂⁺ (m/q 28.0056) and C₂H₄⁺ (m/q 28.0308). The resolution ($m/\Delta m$) is 70,000.

“Land, et al., Rev. Sci. Inst. **61** 1674 (1990).”

29 is the mass of the -CH₂CH₃ group (ethyl), and another at m-90, where 90 is the mass of the OTmSi group (O is oxygen, Si is silicon and Tm stands for trimethyl, (CH₃)₃).

In the lower spectrum all the hydrogen atoms on the ethyl group had deuterium substituted. The peak at m-29 from the upper panel is still there indicating that it has been correctly assigned as has the peak at m-90-29. The peak from (a) at m-90 is now shifted to m-85 since the 5 D-atoms are still present. The two large peaks at lower mass are also shifted up by 5 amu indicating that the ethyl group is still present. The spectrum with the isotope substitution helps definitively identify the molecule.

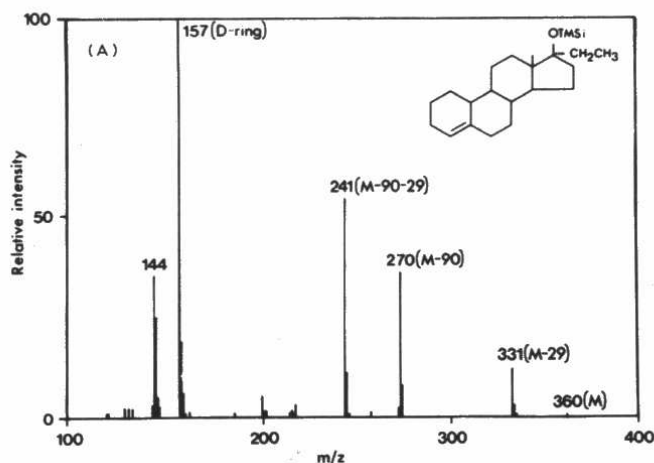
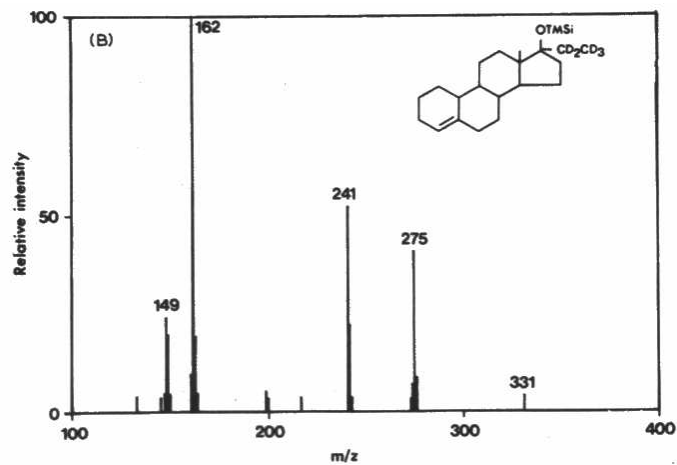


Figure 18: Mass spectra of the TMS ethers of (top) normal and (bottom) deuterium-labeled ethylestrenol. From Bjorkhem et al., *J. Chromatogr. Biomed. Appl.* **232** 154 (1982).



References

- [1] John F. O'Hanlon, "A User's Guide to Vacuum Technology," John Wiley & Sons, New York, 1989.
- [2] Frederick A. White and George M. Wood, "Mass Spectroscopy, Applications and Engineering," John Wiley & Sons, 1986.
- [3] David S. McKay, Everett K. Gison Jr., Kathie L. Thomas-Keprta, Hojatollah Vali, Christopher S. Romanek, Simon J. Clemett, Xavier D. F. Chillier, C. R. Maechling and Richard N. Zare, "Search for Past Life on Mars: Possible Relic Biogenic Activity in Martian Meteorite ALH8," *Science* **273** 5277 (1992).